JOURNAL OF MATERIALS SCIENCE 30 (1995) 5313–5320

Passivity breakdown due to discontinuous precipitation during ageing of 21Cr–10Mn–5Ni stainless steel

I. CHATTORAJ, S. K. DAS*, S. JANA, S. P. CHAKRABORTY*, A. K. BHATTAMISHRA
*CRP Division and *MTP Division, National Metallurgical Laboratory, Jamshedpur, India 831007*

Discontinuous precipitation in a 21Cr–10Mn–5Ni steel was found to result in breakdown of passivity when tested in a 0.5 M H_2SO_4 + 0.01 M KSCN solution. The electrochemical response was similar to that due to sensitization of conventional stainless steels. The ageing time and temperature affected the resistance of the passive film, with lower ageing temperatures being more severe in terms of passivity breakdown. The effect of interlamellar spacing on the chromium depletion, the effect of volume diffusion on the healing of the matrix, and the solubility product reaction for precipitation, were considered to explain the observed different strengths of passive films formed on specimens aged at different temperatures and times. The observance of good corrosion protection in spite of the presence of profuse precipitates was in contrast to the effect of grain-boundary carbide proliferation on the corrosion resistance of conventional stainless steels.

1. Introduction

Discontinuous precipitation is normally associated with the degradation of physical and mechanical properties [1–9] in a wide range of alloys. However, studies on corrosion property changes brought about by such modes of precipitation are few [6–9]. Theoretically, such modes of precipitation become important for the corrosion resistance of austenitic stainless steels because the discontinuous-type chromium carbide precipitate would lead to chromium depletion from localized areas. Whereas the chromium depletion due to grain-boundary carbide precipitation [10–12] and the consequent effects on passivity breakdown [13, 14] have been studied, the significance of discontinuous precipitation *vis-à-vis* the corrosion properties have received little attention, possibly due to the suppression of such reactions in conventional stainless steels and the occurrence of continuous precipitation in preference to discontinuous precipitation. Hillert and Lagneborg [15] had observed lamellar precipitates in their studies on stainless steels subjected to creep. It appears that additional features, such as externally applied strain, are necessary for modifying the nucleation and growth kinetics favourably for discontinuous precipitation in conventional austenitic stainless steels. Faulkner's [16] theoretical developments also show that the breakdown of discontinuous precipitates and the occurrence of continuous precipitates is extremely fast (of the order of a few minutes), thus they possibly avoid detection in industrial situations.

In contrast, the discontinuous precipitates have been observed in substitute stainless steels. Thus in Cr–Mn austenitic stainless steels, Hsiao and Dulis [17] showed that this mode of precipitation was found over a range of temperatures. Nijhawan *et al.* [8] and Henry and Plateau [9] related the observance of discontinuous precipitates to the reduced corrosion resistance of nickel-free stainless steels. Whether the stabilization of the discontinuous precipitate is a result of ternary effects has not been elucidated in these studies. It is clear that the development of substitute stainless steels has been impaired by the occurrence of discontinuous precipitates in addition to the presence of a number of other phases [18, 19].

The process of discontinuous precipitation requires co-operative grain-boundary precipitation and migration [20, 21]. A consequence of such a reaction mechanism is the peculiar solute concentration profile developed near the migrating reaction front [22, 23]. In chromium-containing alloys, if discontinuous precipitation results in local depletion of chromium, a decrease in corrosion resistance is observed; this was best demonstrated in Incoloy 825, which showed rapid intergranular attack after the precipitation of $Cr_{23}C_6$ discontinuous lamellae [6]. The present work addresses the problem of sensitization brought about by discontinuous precipitation in an experimental stainless steel substitute. This attempts to be a systematic study of the effects of isothermal ageing on the strength of passive films formed in a relatively benign media. This article addresses the decrease in corrosion

0022–2461

TABLE I Compositions of the materials used

	Cr	Mn	Ni	Si	S	C	N	Fe
304 Stainless steel	18.8	1.7	9.0	0.33	0.02	0.06	–	Balance
Experimental alloy	20.6	9.7	4.9	0.30	0.02	0.066	0.3	Balance

resistance in terms of the proliferation of discontinuous precipitates and the resultant chromium depletion.

2. Experimental procedure

The materials used in this study had the compositions given in Table I. The experimental alloy was obtained as plates which were hot rolled to a thickness of about 2 mm. Specimens of 25 mm × 25 mm in area were machined from both the alloys and were solution annealed at 1100 °C for 1 h followed by water quenching. With the help of microstructural observations, X-ray diffraction studies and magnetic measurements, it was found that the specimens from both the alloys were fully austenitic after solution annealing. Subsequently they were isothermally aged at different temperatures for different lengths of time followed by water quenching. The aged specimens were ground and polished up to a 0.05 μm finish prior to electrochemical experiments and prior to microscopic observations.

The double-loop potentiokinetic reactivation technique [24] was used to study the localized corrosion due to sensitization of the aged specimens. The potentiokinetic reactivation (PKR) tests were conducted at a potential scan rate of 1.67 $mV s^{-1}$, starting at a potential of − 250 mV with respect to the open circuit potential for the specimen and scanning in the anodic direction up to a vertex potential of 200 mV with respect to a standard calomel reference electrode (SCE). On attainment of the vertex potential (200 mV_{SCE}) the scan was reversed. The specimens were cathodically cleaned at a potential of − 600 mV_{SCE} for 5 min to remove surface oxide films, if any, prior to the PKR tests. The reactivation tests were conducted in a solution of 0.5 M H_2SO_4 + 0.01 M KSCN. After the tests, the samples were rinsed with running water, cleaned with acetone, dried and then observed under a microscope to evaluate the nature and extent of corrosive attack.

To study the microstructural features brought about by ageing, the polished unexposed samples were etched with aqua regia and observed under a scanning electron microscope (SEM). Energy dispersive spectroscopic (EDS) studies revealed the significant enrichment of chromium in the precipitates; however, the limitations of the SEM–EDS prevented the determination of the chromium concentration profile.

3. Results and discussion

In conventional stainless steels (SS), isothermal treatments in the temperature range 600–800 °C lead to chromium depletion near grain-boundaries [10–14] which is termed sensitization and which manifests itself in the inability of such regions to passivate (or in the formation of very weak passive films) in a standard test medium. One electrochemical method for studying and quantifying this process is the potentiokinetic reactivation (PKR) process which entails the specimen being polarized potentiodynamically from a negative overpotential at fixed scan rates to some pre-fixed nobler potential corresponding to the passive region for the material, and then reversing the scan. The rationale for this test is that sensitized specimens will be unable to passivate successfully near grain boundaries depleted of chromium, and this will show up as anodic current peaks in the reverse scans. The details of this method are discussed elsewhere [24, 25]. In our experiments we have used similar cyclic polarization techniques with slight variation in that whereas the conventional technique prescribes holding the specimen for 2 min at the vertex potential after the end of the forward scan, we have resorted to immediate reversal of the potentiodynamic scan. Thus, the weaknesses in the passive film are exposed much more in our method.

In commercial grade 304 SS and other stainless steels, sensitization is a result of grain-boundary precipitation of chromium carbides ($M_{23}C_6$) and has been well documented and extensively studied [10–14]. The nucleation and growth of these precipitates are time- and temperature-dependent. This is very well demonstrated in Fig. 1 where isothermal ageing at 600 °C leads to progressive increase in size and amount of carbides. For the time and temperature combinations tested in this study, no discontinuous-type precipitation was observed in the SS304 material. Although our main aim was to investigate the ability of the experimental alloy (21Cr–10Mn–5Ni) to passivate after isothermal ageing, we also report here the behaviour of commercial 304SS under similar conditions, to provide a comparative estimate of the efficacy of the passive film formed on the experimental alloy.

As stated earlier, the passive film breakdown of 304SS specimens subjected to isothermal ageing conducted during this study was exclusively due to sensitization brought about by grain-boundary precipitation. The electrochemical manifestation of this grain-boundary chromium depletion is depicted in Fig. 2. The degree of sensitization (DOS) which is proportional to the fraction of chromium-depleted boundaries, is popularly expressed by either (i) the ratio of the peak heights of the reverse scan and the forward scan, I_r/I_a, or (ii) the ratio of the areas under the reactivation peak produced on reversing the scan to the area under the peak for the forward scan; these areas are proportional to the total electric charges involved in the respective processes, when the scan

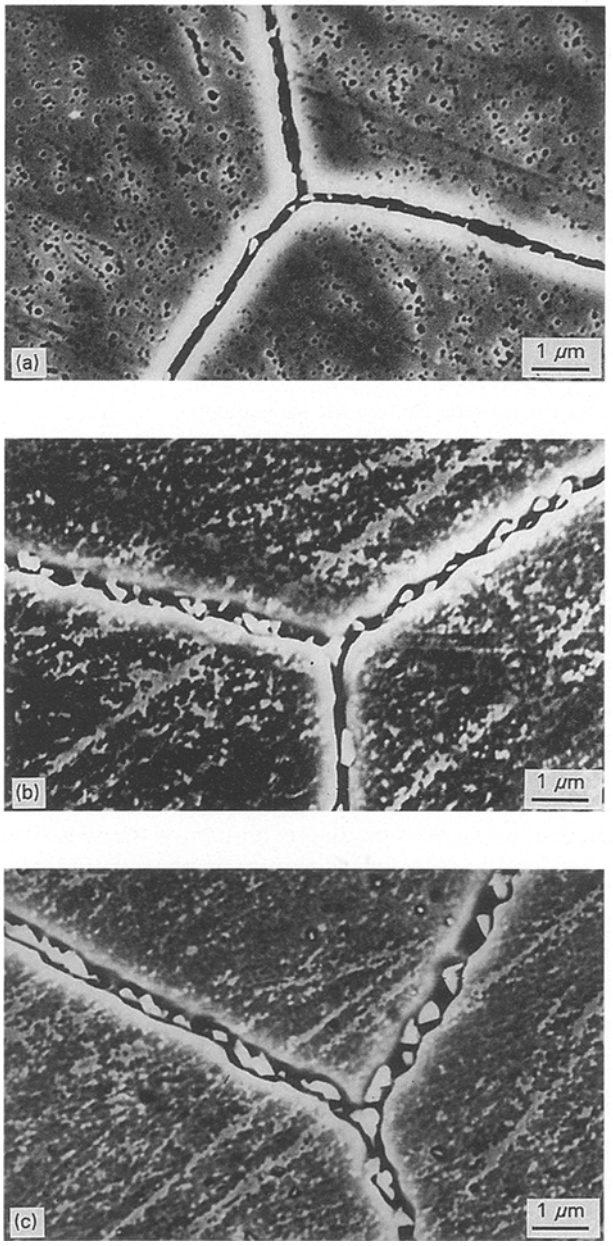

Figure 1 Increase in number and size of grain-boundary carbides on isothermal ageing of SS304 at 600 °C for: (a) 5 h, (b) 24 h and (c) 48 h.

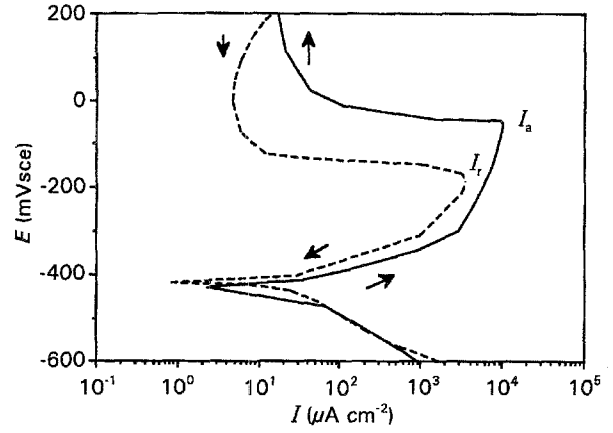

Figure 2 PKR curve for commercial 304 stainless steel material sensitized at 600 °C for 24 h. (——) Forward scan, (– – –) reverse scan.

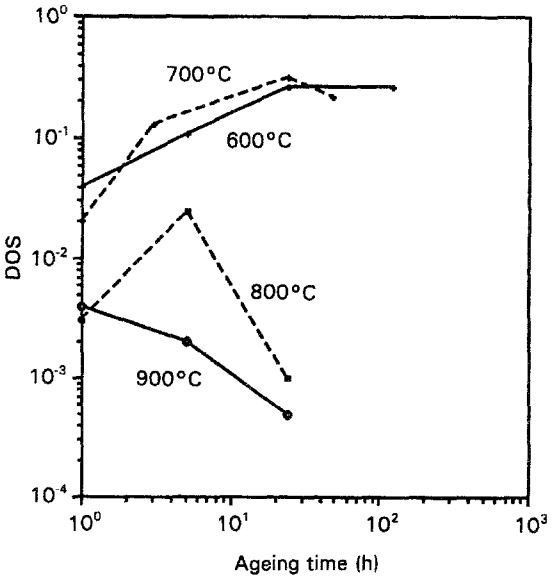

Figure 3 Effect of time and temperature of ageing on the degree of sensitization of 304SS material.

rate is constant. Fig. 3 shows the effect of time and temperature on the DOS values of the stainless steel used. The sensitization is most pronounced at 700 °C, and lower at higher as well as lower ageing temperatures, which conforms to the generally observed [13, 26] "C"-shaped time–temperature–sensitization (TTS) diagrams – a result of the classical dependence of nucleation and growth kinetics in different fashions on the ageing temperature. It should be mentioned here in passing, that the chromium depletion is more or less symmetrical about the grain-boundary precipitates on sensitization of conventional stainless steels [11–13]. This is in contrast to the asymmetrical concentration profile of the solute obtained across any grain-boundary experiencing discontinuous precipitation.

In Cr–Mn and Cr–Mn–Ni steels, discontinuous precipitation and its effect on physical property degradation have been studied by several authors [8, 9, 17]. The lamellar products resulting from this mode of precipitation have been reported to be chromium carbides [17] and for a steel somewhat similar in composition to our experimental alloy, these were found to be chromium carbides and nitrides [9]. The occurrence of discontinuous precipitation in the alloy studied was observed over the temperature range 550–900 °C. EDS analysis of the precipitates showed significant enrichment of chromium and some depletion of nickel and manganese as compared to the matrix. The effect of ageing time was the proliferation of such precipitates on isothermal holding, as shown in Fig. 4. As discussed below, such precipitation (of either carbides, nitrides or carbonitrides of chromium) should cause chromium depletion not only across migrating grain boundaries, but also in the matrix region between precipitate lamellae. It was reasonable to assume that such solute depletion from near-grain-boundary regions would lead to features similar to sensitization in conventional SS. This justified the use of the electrochemical PKR method to study the passive film breakdown in this alloy, apart from reasons of

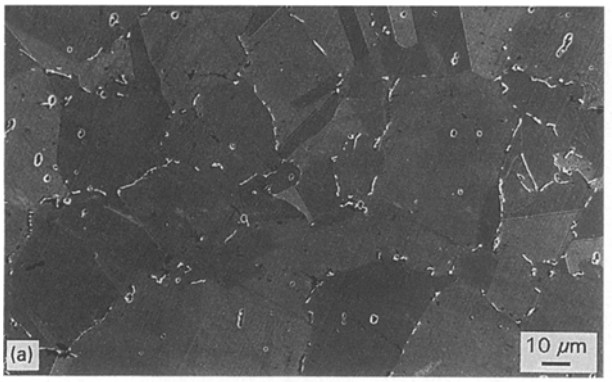

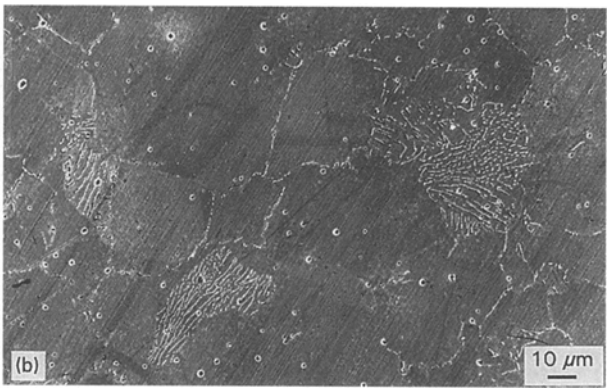

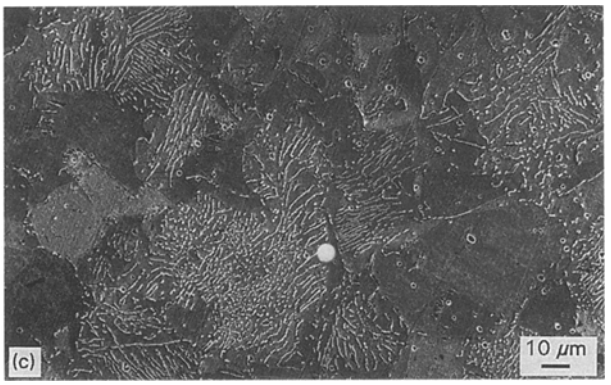

Figure 4 Scanning electron micrographs of the experimental alloy specimens aged isothermally at 800 °C showing increase in discontinuous precipitation with time: (a) 5 h, (b) 24 h, (c) 48 h.

comparison, which were vindicated by the experimental results discussed below. Moreover, although the PKR technique is well suited for the sensitization studies, it is equally useful for characterizing passive films and evaluating the strength of passive films. The results of this cyclic polarization method applied to specimens of the alloy after isothermal ageing are given in Table II. It was observed during the polarization experiments that anodic reactivation loops were demonstrated by specimens aged at 550 and 600 °C for long times. For all ageing times at 650 and 700 °C and for low ageing times at 550 °C, on reactivation, the polarization curves exhibit cathodic loops in the potential ranges that corresponded to the passive potential ranges during the forward scan. On ageing at higher temperatures (800 and 900 °C), the alloy demonstrated passivity on reversing the scan.

The potentiokinetic reactivations show that unlike in 304SS, where a gradual evolution of the sensitization loop is the primary feature, in the experimental alloy, passivity breakdown is more complex. The type of passive film formed can be classified into three groups:

(a) strong passive film, found in specimens aged at high temperatures (800 and 900 °C) and aged for low times at low temperature (550 °C). These are characterized by either the absence of the reactivation loop or the presence of very small loop on reversing the potential scan;

TABLE II The passive film character in 0.5 M H_2SO_4 + 0.1 M KSCN for the 21Cr–10Mn–5Ni steel after different ageing treatments

Ageing temp. (°C)	Ageing time (h)	DOS (from peak heights) I_r/I_a	DOS (from areas under the peaks)	Type of passive film
550	1	0	0	Passive
	7	–	–	(demonstrates cathodic loop)
	16	0.15	0.21	Sensitized
	30	0.31	0.39	Sensitized
600	1	0.01	0.01	Passive
	5	0.01	0.02	Passive
	24	0.3	0.43	Sensitized
	120	0.34	0.24	Sensitized
650	1, 5, 24	–	–	(Demonstrates cathodic loop)
700	1, 5, 24, 48	–	–	(Demonstrates cathodic loop)
800	1	0.001	–	Passive
	5	0.003	–	Passive
	24	0.005	–	Passive
	48	0.07	–	Passive
900	1	~ 0	–	Passive
	24	0.001	–	Passive
	48	0.002	–	Passive

(b) sensitized passive film, where the matrix region near the grain boundaries is incapable of passivation thus demonstrating a significant reactivation loop. This behaviour is observed for specimens aged for long times at 550 and 600 °C;

(c) weak passive film, found on specimens aged at 650 and 700 °C. These demonstrate a cathodic loop as well as anodic reactivation loop on reversing the scan.

Representative polarization curves for these groups are shown in Fig. 5 and we will attempt to explain these variations in terms of the electrochemical processes occurring on the alloy surface and then correlate them to the microstructural features and resulting chromium depletion brought about by discontinuous precipitation.

The polarization curves for strongly passive films and sensitized films (Fig. 5a and b, respectively) are self explanatory. The occurrence of a cathodic loop in the PKR curve (Fig. 5c) indicates dissolution of the surface oxide (passive film) by reduction. Subsequently, in the absence of a protective film, the surface undergoes anodic dissolution in the potential range conducive for this phenomenon. It is not possible to specify from the PKR curves of the third type whether the passive film dissolution is local (that is, restricted to grain boundaries, precipitate–matrix interface and solute

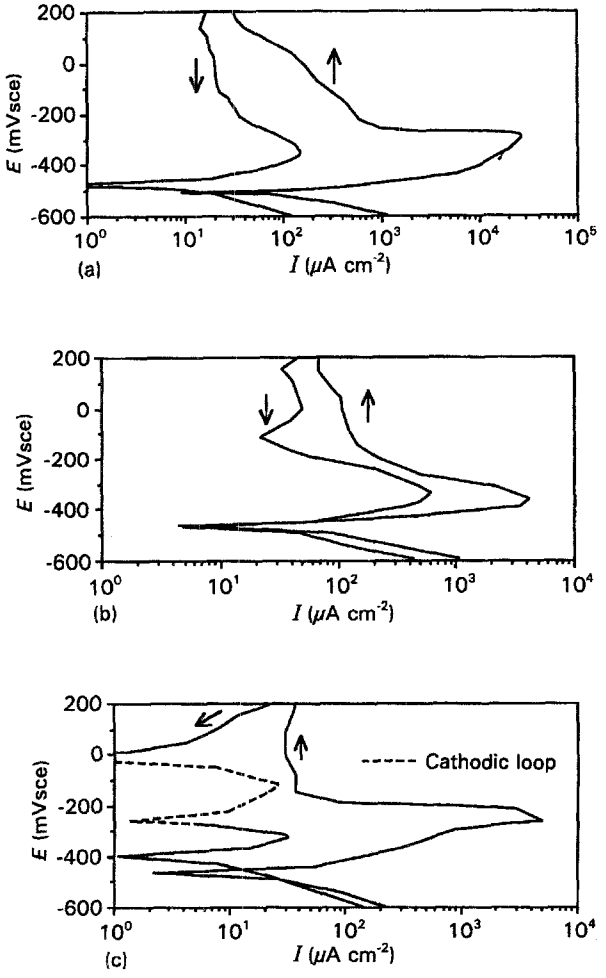

Figure 5 PKR curves for the experimental alloy for three different ageing conditions showing different passive film strengths: (a) 900 °C for 24 h, (b) 550 °C for 16 h, and (c) 700 °C for 24 h. (– – – –) Cathodic loop.

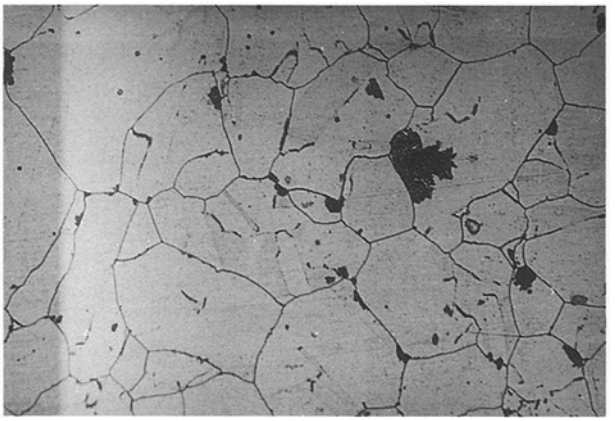

Figure 6 Post-PKR micrograph of specimen aged at 650 °C for 24 h prior to the PKR test.

depleted matrix), or general. Post-PKR microstructural observation shows preferential attack of the regions near grain boundaries (Fig. 6), thus the passive film breakdown occurs over local areas. Interpretation of this third type of PKR curve is further complicated by the fact that simultaneous oxide reduction and anodic dissolution of the bare surface is possible, and polarization experiments can only indicate the difference in the reaction rates of the anodic and cathodic processes at any applied potential without providing any information on the individual reaction rates. Thus the relative strength and weakness of the passive films on specimens exhibiting cathodic loops on reactivation cannot be assessed.

The electrochemical data show that specimens aged at 550 °C for 1 h develop a strong passive film and those aged for long times (16 and 30 h) are sensitized. The weak passive films developed at intermediate ageing times at this temperature indicate a transition towards local susceptibility brought about by the gradual depletion of chromium with time from such areas. This transition is from strong passive films for specimens aged for 1 h to sensitized films for specimens aged for long times at 600 °C, without the demonstration of weak passivity at intermediate ageing times. For specimens aged at 650 and 700 °C, the passive film formed is weak, for all ageing times investigated. Thus ageing in the temperature range 550–700 °C for sufficient time, causes the passive films formed during subsequent electrochemical polarization to be quite weak or absent near the grain boundaries. An anomaly is evident in the degree of sensitization calculated for the specimens aged at 600 °C by the two methods. Whereas the ratio of the peak heights suggest similar DOS for specimens aged for 24 and 120 h, the ratio of the peak areas show a decrease in DOS for the specimens aged for higher times. Because the latter method takes into account the cumulative effect of the entire potential range over which anodic dissolution occurs, this should be more reliable. The decrease in DOS is similar to desensitization reported in stainless steels brought about essentially by a change in the chromium activity, and it is reasonable to assume such desensitization mechanisms operating in our alloy. The commercial SS tested

showed such desensitization on long-term ageing at 600 °C as well as 700 °C (Fig. 3).

Discontinuous precipitation, although having some features in common with grain-boundary precipitation, also introduces additional physical and chemical features and artefacts which affect the electrochemical response of the alloy. The salient features of discontinuous precipitation have been reviewed comprehensively [1]. In this particular alloy, the discontinuous reaction is a Type 1 reaction [1, 27] represented by $\gamma \rightarrow \gamma' +$ precipitate, where γ' is the chromium-depleted austenite matrix. Discontinuous precipitation necessitates simultaneous grain-boundary migration and precipitation. A consequence of this is an asymmetrical concentration profile across the migrating grain-boundary with a discontinuous change in solute concentration from a high value in the untransformed grain to a low value in the adjacent transformed grain. The concentration of chromium in between the lamellae should thus be of uniform low value; however, theoretical considerations [16] show that a local maximum should occur at half the interlamellar spacing. While the chromium concentration profile is symmetrical about the grain-boundary precipitate; the same for the alloy investigated would be dictated by the superposition of two perpendicular profiles, the profile across the grain-boundary dictated by grain-boundary diffusion of chromium and the profile between two precipitate lamella. Local minima in concentration would exist at the precipitate–matrix interfaces and the grain-boundary-depleted matrix interfaces; these regions would thus be expected to be most susceptible to electrochemical attack. Because a role of the interlamellar spacing is suggested, we investigated its variation with different ageing temperatures (Table III). The spacing is time-independent and depends only on the ageing temperature, as shown in Fig. 7.

Whereas the lamella–matrix interface was expected to be susceptible to localized corrosion, post-PKR microscopic observations show that such susceptibility is low and anodic dissolution occurs mostly near grain boundaries (Figs 6 and 8). That the specimens aged at 650 °C are not sensitized is seen by comparing the grain-boundary width after the PKR experiment (Fig. 6) with that of a sensitized specimen (Fig. 8). In addition, the interlamellar matrix is relatively free of corrosive attack. The presence and proliferation of discontinuous precipitates do not necessarily imply increased attack, as demonstrated by the strong passivity of specimens aged at 800 °C which have significant precipitate colonies (Fig. 4) and also by the decrease in sensitization in spite of the increased volume fraction of precipitates observed on ageing for 120 h at 600 °C as compared to ageing for 24 h. These observations indicate opposing forces operating to influence the chromium concentration profile.

The high susceptibility of specimens aged at low temperatures is primarily due to the lower interlamellar spacing. The spacing essentially decides the number of sinks in a given volume of material for chromium depletion from the matrix through the grain-boundary route. The relative insensitivity of the lamellae–matrix interface regions away from the migrating grain boundaries is due to the opposing influence of volume diffusion of chromium tending to smoothen the concentration gradients, so that only the chromium-depleted grain-boundary–matrix interfaces

TABLE III The variation of interlamellar spacing with ageing temperature for the experimental alloy

Ageing temperature (°C)	600	700	800	900
Interlamellar spacing, S (μm)	0.5	1.1	2.5	4

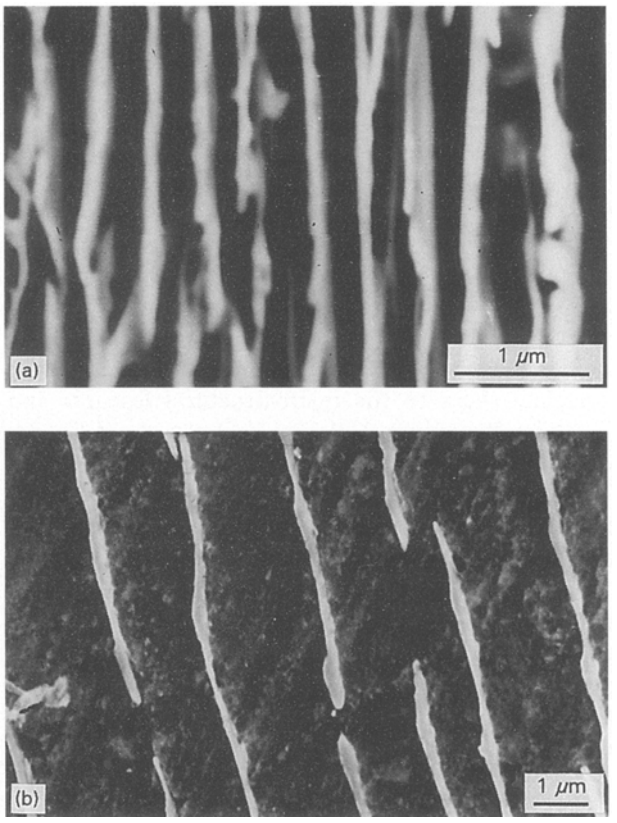

Figure 7 Effect of temperature on the interlamellar spacing in between the discontinuous precipitate: (a) aged at 600 °C for 120 h, and (b) 800 °C for 48 h.

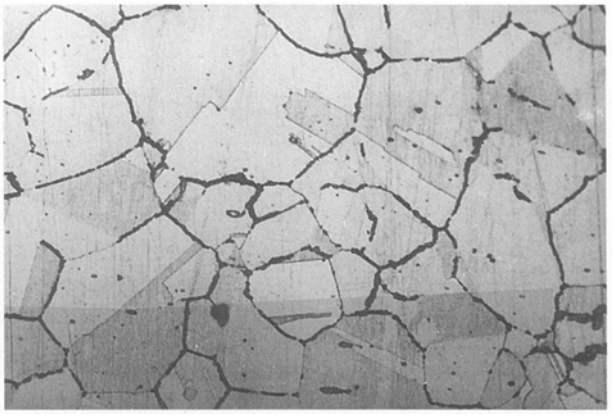

Figure 8 Post-PKR micrograph of specimen aged at 600 °C for 120 h prior to the PKR test.

and the lamellae–matrix interfaces close to the grain boundaries are attacked. These features are elaborated below.

The effect of interlamellar spacing is evident from a simple exercise in mass balance for chromium. If the interlamellar spacing is S and the precipitate particle radius is r_p, then considering a cuboid around a single precipitate of unit length and with S being the other dimensions, on applying chromium balance we obtain

$$S^2\delta C_{GB} + \pi r_p^2 C_p = (C_0 - C_{avg})(S^2 - \pi r_p^2) \quad (1)$$

where C_p, C_0, C_{avg} and C_{GB} are the chromium concentrations in the precipitate, in the untransformed matrix, the average value for the depleted interlamellar matrix, and the chromium content in the grain boundaries, respectively, and δ is the grain-boundary thickness. Because the reported values of δ ($\sim$0.2 nm) are much smaller than the other dimensions, the first term in the equation can be neglected, giving

$$[C_p + C_0 - C_{avg}]/(C_0 - C_{avg}) = S^2/\pi r_p^2 \quad (2)$$

because typically $C_p + C_0$ ($=K$) $\gg C_{avg}$ for the depleted matrix

$$C_0 - C_{avg} = K\pi r_p^2/S^2 \quad (3)$$

While Equation 3 provides the average chromium depletion, the concentration profile is decided by the growth kinetics and by the thermodynamics of the precipitate-forming reaction. In the case of formation of $Cr_{23}C_6$ precipitates, the equilibrium reaction is $23Cr + 6C = Cr_{23}C_6$, so that the equilibrium chromium concentration at the particle–matrix interface, C_E, is given by

$$(C_E)^{23} a_c^6 = \exp(-\Delta G/RT) \quad (4)$$

where a_c is the activity of carbon and the other terms have conventional meanings. An understanding of the ageing temperature effect can be obtained from Equation 4 which clearly shows the temperature dependence of C_E. Because a_c decreases with ageing time [16], C_E would increase with time on isothermal ageing, thus providing healing to the depleted matrix. It is clear from Equation 3 that the total chromium depletion is dependent primarily on the ageing temperature, because S is time-invariant and the increase in particle radius, r_p, is slight with ageing time for essentially unidirectional growth observed during discontinuous precipitation. Thus, at lower ageing temperatures, lower interlamellar spacings would cause increased chromium depletion; also C_E is smaller compared to higher temperatures, which means that the particle–matrix interface would be more susceptible for specimens aged at lower temperatures. One effect of ageing time is the increase of the volume fraction, demonstrating discontinuous precipitates. On the other hand, C_E would tend to decrease with ageing. Thus the electrochemical responses observed are a result of these counteracting influences; the former would create more grain boundaries depleted of chromium, the latter would reduce the susceptibility of individual grain boundaries by altering the concentration profiles favourably. It is evident from the preceding discussion that lower ageing temperatures would be more detrimental to passive film stability, as borne out by the experimental results presented earlier (Fig. 5 and Table I). A lower limit to the detrimental ageing temperature would be due to the reduced nucleation of discontinuous precipitates.

TABLE IV Chromium concentration average values for depleted interlamellar matrix

Ageing temperature (°C)	700	800	900
C_{avg} (wt %)	12.3	19.5	19

Using the data obtained from SEM for r_p and S and from the EDS for C_p (0.45 $\pm$ 0.05 weight fraction chromium), we calculated the C_{avg} values at different ageing temperatures with the help of Equation 2. The C_p value was found to be unaffected by changing ageing parameters. It was also observed that in addition to chromium, other metallic elements namely iron, nickel and manganese were also present in the precipitate. Applying chromium balance only, the C_{avg} values given in Table IV were obtained. At lower ageing temperatures, Equation 2 becomes invalid because the contribution of the first term in Equation 1 cannot be neglected. This does not detract from the earlier observation that chromium depletion is higher at lower temperatures, as a consideration of Equation 1 will reveal. The calculated average chromium contents of the interlamellar matrix show the healing effect of higher temperature ageing. For austenitic stainless steels, a value of 13% Cr is generally found to provide stable passive film. The observation of weak passivity of the materials aged at 700 °C is thus explained, so is the immunity to corrosive attack of the specimens aged at higher temperatures. It should be stated that Equation 4 is strictly valid when the precipitates contain only chromium as the metallic element. In the case of intermetallic carbides and nitrides, suitable activities of the other elements have to be included in the solubility product equation.

The observation of the relative independence of sensitization from the volume fraction transformed can be partly attributed to the changing values of C_E with time, discussed earlier. The second factor is the

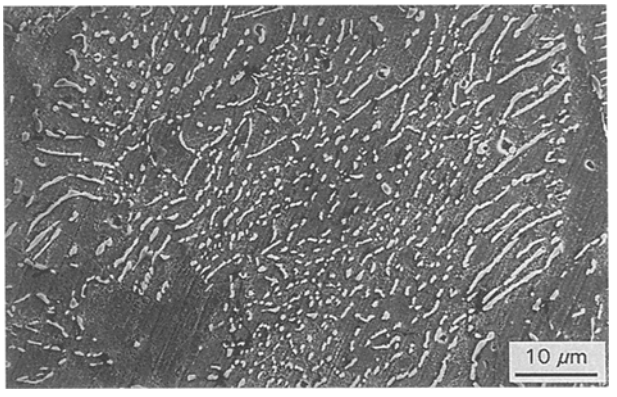

Figure 9 Redissolution and spheroidization of lamellar precipitates on ageing at 800 °C for 48 h. (This micrograph corresponds to the region near the circular white spot in Fig. 4c.

homogenizing influence of volume diffusion, which is most evident at high temperatures where discontinuous precipitation breakdown and change over to continuous precipitation occurs [17]. The redissolution and spheroidization of lamellae shown in Fig. 9 is evidence of such a process. At long ageing times, the matrix in between parts of the lamella far removed from the migrating grain boundaries would be subject to the influence of volume diffusion. The result is that only the interlamellar matrix close to the grain boundaries is substantially depleted of chromium to show up as being sensitized during electrochemical experiments.

4. Conclusions

1. Discontinuous precipitation in a 21Cr–10Mn–5Ni steel resulted in breakdown of passivity during subsequent electrochemical experimentation. Three types of passive films could be classified and their occurrence depended on the time and temperature at which the specimen had been aged.

2. The deleterious effect of low-temperature ageing could be correlated to the decreased interlamellar spacings of the discontinuous precipitate. Theoretical developments along the lines of chromium mass balance between the precipitate and the matrix, and the calculated values of the average chromium depletion from the interlamellar matrix showed the effects of ageing temperature on chromium depletion.

3. An increase in discontinuous precipitate colonies did not necessarily result in decreased corrosion resistance, which could be explained by the changing activity of chromium with time which affected the chromium concentration profile, as well as by the effect of volume diffusion.

Acknowledgements

The authors thank the Director, National Metallurgical Laboratory, for his permission to publish this article. The help and advice provided by Dr Inder Singh and by Messrs P. K. De, B. N. Ghosh, S. B. Tiwari and Niranjan Das, are gratefully acknowledged.

References

1. D. B. WILLIAMS and E. P. BUTLER, *Int. Met. Rev.* **3** (1981) 153.
2. R. O. WILLIAMS, *Trans AIME* **215** (1959) 1026.
3. M. KORCHYNSKY and R. W. FOUNTAIN, *ibid.* **215** (1959) 1033.
4. R. B. SCARLIN, *Scripta Metall.* **10** (1976) 711.
5. S. I. NISSAN, Y. KOMEN and B. Z. WEISS, *Acta Metall.* **23** (1975) 1313.
6. E. L. RAYMOND, *Corrosion* **24** (1968) 180.
7. R. CHAIT and P. LUM, *ibid.* **32** (1976) 450.
8. B. R. NIJHAWAN, P. K. GUPTE, S. S. BHATNAGAR, B. K. GUHA and S. S. DHANJAL, *J. Iron Steel Inst.* **205** (1967) 292.
9. G. HENRY and J. PLATEAU, *NML Tech. J.* **5** May (1963) 25.
10. C. STAWSTROM and M. HILLERT, *J. Iron Steel Inst.* **207** (1969) 77.
11. E. L. HALL and C. L. BRIANT, *Metall. Trans.* **15A** (1984) 792.
12. G. S. WAS and R. M. KRUGER, *Acta Metall.* **33** (1985) 841.
13. S. M. BRUEMMER, L. A. CHARLOT and B. W. AREY, *Corrosion* **44** (1988) 328.
14. T. M. DEVINE, *J. Electrochem. Soc.* **126** (1979) 374.
15. M. HILLERT and R. LAGNEBORG, *J. Mater. Sci.* **6** (1971) 208.
16. R. G. FAULKNER, *Mater. Sci. Technol.* **9** (1993) 118.
17. C. HSIAO and E. J. DULIS, *Trans. ASM* **49** (1957) 655.
18. A. J. SEDRIKS, *Corrosion* **45** (1989) 510.
19. A. M. RITTER and M. F. HENRY, Metall. Trans. **16A** (1985) 1759.
20. K. N. TU and D. TURNBULL, *Acta Metall.* **15** (1967) 369.
21. R. A. FOURNELLE and J. B. CLARK, *Metall Trans.* **3** (1972) 2757.
22. E. HORNBOGEN, *ibid.* **3** (1972) 2717.
23. D. A. PORTER and J. W. EDINGTON, *Proc. R. Soc.* **A358** (1977) 335.
24. W. L. CLARK, V. M. ROMERO and J. C. DANKO, "Corrosion/77", paper 180 (NACE, Houston, TX, 1977).
25. A. P. MAJIDI and M. A. STREICHER, *Corrosion* **40** (1984) 584.
26. T. A. MOZHI, W. A. T. CLARK, K. NISHIMOTO, W. B. JOHNSON and D. D. MACDONALD, *ibid.* **41** (1985) 555.
27. M. N. THOMPSON, PhD thesis, Univeristy of Cambridge (1971).

Received 16 September 1993
and accepted 17 May 1994